Surface regulation with polymerized small molecular acceptor towards efficient inverted perovskite solar cells

Dongyang Li, Yulan Huang, Ruijie Ma, Heng Liu, Qiong Liang, Yu Han, Zhiwei Ren, Kuan Liu, Patrick Wai-Keung Fong, Zhuoqiong Zhang, Qing Lian, Xinhui Lu, Chun Cheng* and Gang Li**

D. Li, Y. Huang, Z. Zhang, Q. Lian, Prof. C. Cheng, Department of Materials Science and Engineering, Southern University of Science and Technology, Shenzhen, Guangdong Province, 518055 China
Email: chengc@sustech.edu.cn

D. Li, Dr. R. Ma, Q. Liang, Y. Han, Dr. Z. Ren, Dr. K. Liu, Dr. P. Fong, Prof. G. Li, Department of Electronic and Information Engineering Research Institute for Smart Energy (RISE), The Hong Kong Polytechnic University, Hung Hom, Kowloon, Hong Kong, China
Email: ruijie.ma@polyu.edu.hk; gang.w.li@polyu.edu.hk

H. Liu, Prof. X. Lu, Department of Physics, The Chinese University of Hong Kong, New Territories, Hong Kong, China

Prof. G. Li, Shenzhen Research Institute, The Hong Kong Polytechnic University, Shenzhen, Guangdong, 518057 China

Prof. C. Cheng, Guangdong Provincial Key Laboratory of Energy Materials for Electric Power, Southern University of Science and Technology, Shenzhen 518055, China

Prof. G. Li, Guangdong-Hong Kong-Macao (GHM) Joint Laboratory for Photonic-Thermal-Electrical Energy Materials and Devices, The Hong Kong Polytechnic University, Hung Hom, Kowloon, Hong Kong, 999077, China.

Abstract

Optimizing the interface between the perovskite and transport layers is an efficient approach to promote the photovoltaic performance of inverted perovskite solar cells (IPSCs). Given decades of advances in bulk materials optimization, the performance of IPSCs has been pushed to its limits by interface engineering with a power conversion efficiency (PCE) over 25% and excellent stability most recently. Herein, a celebrity n-type polymeric semiconducting material, PY-IT, that has shown remarkable performance in organic photovoltaics, is introduced as interface regulator between perovskite and ETL. Encouragingly, this polymerized small molecular acceptor (PSMA) exhibits significant effectiveness in both passivation defects and electron transfer facilitation properties on merits of strong planarity and rotatable linkers, which significantly optimized perovskite grain growth orientation and added charge transport channels. As a result, the PSMA-treated IPSC devices obtain an optimal efficiency of 23.57% with a FF of 84%, among the highest efficiency among PSMA-based IPSCs. Meanwhile, the photo-stability of PSMA devices is eye-catching, maintaining ~80% of its initial PCE after 1000 hour of simulated 1-sun illumination under maximal power point (MPP) tracking. This work combines the achievements of polymer science and IPSC device engineering to provide a new insight into interface regulation of efficient and stable devices.

Keywords: Inverted perovskite solar cells, polymerized small molecular, surface reconstruction

1. Introduction

Over the last decade, organic-inorganic metal halide perovskite solar cells (PSCs) have been extensively researched and demonstrated an unprecedented improvement in power conversion efficiency (PCE).[1] Though regular devices (n-i-p) have kept the record PCE values for single-junction PSCs these years, it is widely acknowledged that inverted PSCs (p-i-n) are more promising in the future, due to their negligible hysteresis, and easily large-scale fabrication, and compatibility with flexible substrates and tandem configurations.[2] Therefore, pushing the PCE and stability of IPSCs to a higher level is still the priority in this research field.[3]

The reasons for limited PCE in IPSCs are mainly recognized to be: (i) serious non-radiative recombination caused by defects on film surfaces and grain boundaries; (ii) poor energy level alignment between electron transport layers (ETL), such as PCBM and C_{60}, and perovskite active layers.[4] To simultaneously address these issues, materials that can passivate the defects and adjust the energy level distribution are highly desired.[5] Compared with traditional passivators that cannot passivate two kinds of defects at the same time, conjugated organic semiconducting small molecules have gradually taken the dominant position as effective passivators.[6] Specifically, small molecular acceptors with ring fusion developed from the field of organic photovoltaics (OPVs), including ITIC, IT-M, IT4F, Y6, etc.,[7] have been proven to be good candidates. However, these small molecules are found to be intrinsically fragile in film and unstable under continuous operation, which would restrict the further development of IPSCs: from rigid to flexible, from unstable to stable.[8]

Drawing on the development of OSCs material design and synthesis, a novel concept of polymeric small molecule acceptor (PSMA) has been proposed in recent years.[9] These kinds of materials can be efficient in charge transport as small molecules are, and stable as polymers.[10] Therefore, PSMAs are not only efficient in constructing all-polymer OSCs, but also promising in regulating the perovskite/ETL interface properties as a multi-functional passivators, thereby enhancing the PCE and stability of

IPSCs. Besides, the use of PSMA as a passivator has not been reported in the field, which may open up a new direction of perovskite passivation engineering.[11]

In this work, we reported a surface reconstruction strategy by the incorporation of a PSMA named PY-IT, which created record efficiency in all-polymer OSCs.[12] The PY-IT acts as the perovskite/ETL interface modulator to reduce defect states and enhance electron extraction/transfer for highly efficient IPSCs. It is found that PY-IT is mainly distributed at the top surface of perovskite, where it functions in three ways. First, its functional groups can interact with undercoordinated Pb^{2+}, providing strong passivation effect of the defects of the perovskite film and effectively suppressing the non-radiative recombination.[13] In addition, the n-type property of PSMA promotes electron transport between perovskite and ETL.[14] Furthermore, due to the molecular interaction with perovskite, the localization of PY-IT on the surface is long-range ordered and intrinsically face-on oriented, which is also beneficial for electron transport between the perovskite and ETL.[12a, 15] Upon the powerful regulation, the PSMA-treated IPSCs yielded a champion PCE of 23.57% with an outstanding fill factor (*FF*) of 84% compared to the control (21.96%) for 1.53 eV perovskite system. In addition, the PSMA-incorporated IPSCs retained 86% and 80% of their initial PCE storing in N_2 atmosphere (unencapsulated) and light soaking in air (encapsulated and under maximal power point tracking) for 1000 h, respectively. These are also far more excellent than those of counterparts. Furthermore, this strategy is potentially generally applicable, supported by the increase of PCE of narrow bandgap system ($Cs_{0.1}FA_{0.6}MA_{0.3}Pb_{0.5}Sn_{0.5}I_3$, 1.25 eV), from 17.38% to19.62% after PSMA treatment. All in all, the performance of IPSCs was significantly improved by rationally selecting passivation materials, regardless of the composition of perovskites. This provides a new direction for perovskite/ETL interface manipulation and demonstrates an encouraging case of successfully combining results from two fields: OPV material science and PSC devices engineering.

2. Results and discussion

The chemical structure of PY-IT is shown in **Figure 1a**, in which the S, N and O contained functional groups with high electron density are supposed to play as Lewis base to passivate undercoordinated Pb^{2+} in perovskite films.[4a, 6b] To prepare the IPSCs with PSMA, the $Cs_{0.05}(FA_{0.98}MA_{0.02})_{0.95}Pb(I_{0.98}Br_{0.02})_3$ perovskite layer was first fabricated via one-step antisolvent method. Then, PY-IT was dropped on the perovskite surface by spin coating, combined with thermal annealing to enable effective interaction. Hereafter, the perovskite films with PY-IT are denoted as PSMA for simplicity.

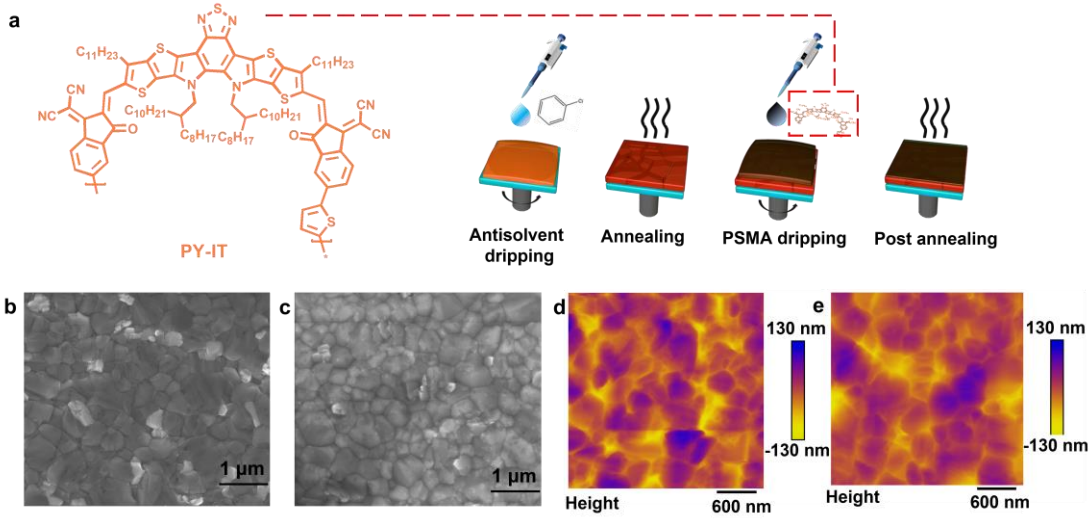

Figure 1. (a) Chemical structure of PY-IT and schematic illustration of film deposition procedure. (b) Top-view SEM images and AFM height images of the (b, d) control and (c, e) PSMA-perovskite films.

2.1 PSMA-induced surface reaction

The morphology is first performed using scanning electron microscopy (SEM) to explore the effect of PSMA surface treatment. As shown in **Figures 1b** and **1c**, both samples displayed clear perovskite grains with obvious grain boundaries and white Pb-rich phase, indicating well-prepared perovskites with high crystallinity.[16] However, the perovskite film tended to be blurred and to have strips on the surface after PSMA treatment, which suggests that PY-IT has been successfully coated and attached on the surface of perovskite film.[7c] The atomic force microscopy (AFM) images of the two

perovskite films displayed grain sizes ~600 nm (**Figures 1d and 1e**), consistent with the SEM results. In addition, the root-mean-square roughness of the control film (33.0 nm) was much higher than that of the PSMA-modified counterpart (22.5 nm), indicating that the film became more uniform after the incorporation of PSMA.[17] These results imply that the PSMA modification has negligible effect on the perovskite grain size but significantly reduces the surface roughness. Therefore, PY-IT is supposed to be located at the grain boundaries and possibly enriched on the top of perovskite film. To verify this hypothesis, the time-of-flight secondary-ion mass spectroscopy (ToF-SIMS) of both samples were conducted with the structure of ITO/SAM/perovskite (with or without PY-IT). As shown in **Figures 2a** and **2b**, the intensity traces of S^-, PbI^-, PO_3^-, and InO^- are performed on both control and PSMA modified films, which refer to the component of PY-IT, perovskite, 2PACz (self-assemble monolayer: SAM), and ITO electrode, respectively. The 3D signal distribution of segments was also presented in **Figure S1**. Based on the signal intensity along with sputtering time, we could have a well understanding of the vertical distribution of PY-IT and perovskite. The signal of S^- in the PSMA-modified film appeared in the first 60s of sputtering, proving the enrichment of PY-IT on the top part of perovskite film. Specifically, after a rapid drop in the S^- signal at the beginning, the reduction rate became slower from 10 s to 60 s sputtering time, which implies that this PSMA penetrated into the bulk (probably located at grain boundaries).[7a]

One step further, X-ray photoelectron spectroscopy (XPS) was employed to investigate the interaction between perovskite and PY-IT. XPS spectra showed that the S 2p peak can be observed ~ 165 eV for PSMA-treated film, further confirming the presence of PSMA (**Figure 2c**).[18] Interestingly, compared to the control, the slightly downshifted binding energy of Pb 4f at 143 eV and 138 eV could be attributed to the interaction between undercoordinated Pb^{2+} and electron-rich groups (C-N, C=O and thiophene) (**Figure 2d**).[19] Moreover, Fourier transform infrared spectroscopy (FTIR) was conducted to confirm the interaction between the PSMA and perovskite (**Figure S2**). As shown in **Figure 2e**, the stretching vibration peak of C=O shifted from 1690

cm^{-1} for PSMA to 1694 cm^{-1} for PSMA-PbI_2 and the stretching vibration peak of C≡N shifted from 2214 cm^{-1} for PSMA to 2218 cm^{-1} for PSMA-PbI_2, representing a significant interaction between perovskite and the PSMA.[20] These characterizations well elucidate the distribution of the PSMA and its interaction with perovskite.

To figure out the opto-electronic property and morphology tuning effect of PSMA passivation strategy, ultraviolet visible absorption (UV-Vis) and X-ray diffraction (XRD) measurements were performed. As shown in **Figure 2f** and **Figure S3**, the UV-Vis absorption spectra and XRD patterns showed similar characteristics of the control and PSMA perovskite films. The optical bandgap of both perovskite films was 1.53 eV. Besides, the characteristic XRD peaks of both perovskite films remained unchanged, which is consistent with the fact from SEM and AFM results.[21] However, the grazing-incidence wide-angle X-ray scattering (GIWAXS) results showed that the notable diffraction peak at 0.85 $Å^{-1}$ (**Figures 2h** and **2i**), corresponding to the hexagonal non-perovskite δ phase of $FAPbI_3$ in the control film, could be fully eliminated by PSMA treatment.[22] Besides, the intensity of (100) peak of PSMA-treated film at 1.02 $Å^{-1}$ is significantly improved, demonstrating that the upper part of perovskite film has more face-on orientation (**Figure 2j**).[12a, 23] A slightly decreased peak of PbI_2 could also be observed at 0.94 $Å^{-1}$ after PSMA treatment(**Figure S4**), which might be related to the formation of amorphous PSMA-PbI_2 compounds, further supporting the interaction between perovskite and PSMA.[24] The more face-on orientated upper active layer is suggested to provide more electron transport channels, enhancing the charge transport and extraction.[25] Moreover, the contact angle is shown in **Figure S5**, the results show that more hydrophobic surface of PSMA treatment (27° for control and 70° for PSMA), confirming the presence and improved moisture resistance.[26]

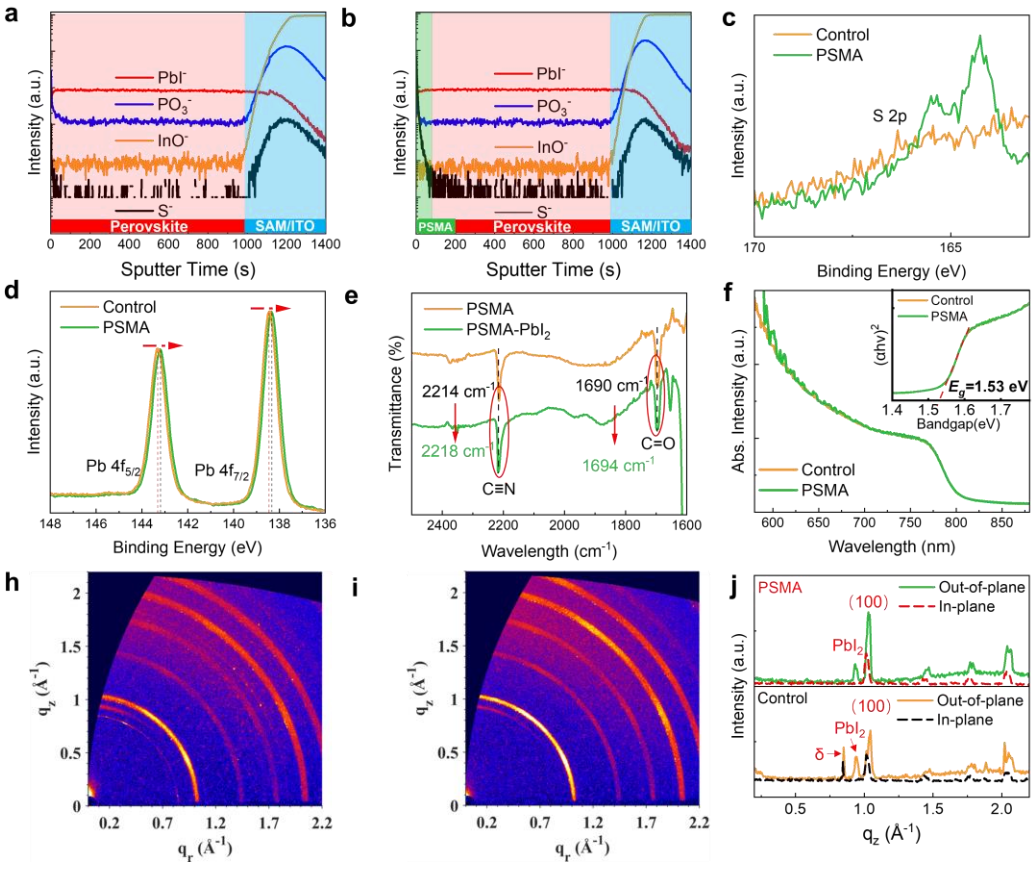

Figure 2. ToF-SIMS profiles of (a) control and (b) PSMA perovskite films. XPS spectra of (c) S 2p and (d) Pb 4f of control and PSMA perovskite films. (e) FTIR spectra of PSMA and PSMA-PbI_2. (f) UV-Vis of control and PSMA perovskite films. The insert is the derived Tauc-Plots. 2D GIWAXS patterns of (h) control and (i) PSMA perovskite films, and (j) corresponding in-plane and out-of-plane line-cuts.

2.2 Carrier dynamics with PSMA

Steady-state photoluminescence (PL) and time-resolved photoluminescence (TRPL) spectroscopy were performed to investigate the defect passivation and electron transport.[27] In the steady-state PL spectra (**Figure 3a**), the PL quenching of PSMA-treated perovskite film was observed compared to the initial control film, demonstrating efficient charge transfer at the perovskite/PSMA interface. In addition, the initial perovskite film produced a PL emission peak ~802 nm, which was shifted to 799 nm after PSMA modification, indicating reduced defects by effective passivation.[28] According to the TRPL spectra (**Figure 3b and Figure S6**) for control and PSMA;

perovskite/PCBM and perovskite-PSMA/PCBM, the nonradiative recombination caused by the interface (τ_1, fast decay lifetime) and the radiative recombination in the bulk perovskite (τ_2, slow decay lifetime) could be evaluated. The fitted parameters were listed in **Table S1**. The fast decay lifetime dominated in both control and PSMA-treated perovskite films, suggesting that nonradiative recombination is the main factor of performance loss. The carrier lifetime reduced from 323 ns for control to 89 ns for PSMA-coated perovskite film, supporting the effectiveness of PY-IT passivation that enabled faster charge transfer and suppressed non-radiative recombination.[4f, 27, 29]

Next, ultraviolet photoelectron spectroscopy (UPS) was measured to evaluate the energy band structure (**Figure 3c**). The PSMA-treated perovskite exhibited a sharp upward shift of the Fermi level (E_F) from -4.87 eV (control) to -4.53 eV, indicating more n-type perovskite surface and thus favorable for electron extraction.[30] To confirm that a more n-type surface was obtained, Kelvin probe force microscopy (KPFM) measurements were conducted to observe the electrostatic potential distribution. The average potential of the control film was -430 mV (**Figure 3d**), higher than that of the PSMA-treated film (-400 mV) (**Figure 3e**), consistent with UPS results. The KPFM image of the control film exhibited clear edges associated with the inhomogeneous surface potential of perovskite film, where detrimental defects existed. In contrast, for the PSMA-treated perovskite film, it showed a more uniform distribution of potential (less fluctuation), suggesting a reduction in local surface defects.[31] In addition, combined with the above AFM results, the perovskite/ETL interface is smoother and has fewer defects, which could benefit the electrons extraction. Furthermore, the high electron affinity of PY-IT with PCBM can promote fast electron transport from perovskite with improved electron channels from GIWAXS results.[32]

Based on the space charge limited current (SCLC) methods, electron-only devices were fabricated using the structure of ITO/SnO_2/active layer/PCBM/BCP/Ag with or without PSMA treatment to further investigate the effectiveness of surface passivation. The transition voltage from the ohmic region to the trap-filling limit region is referred to the trap-filling limit voltage (V_{TFL}), and it is associated to the trap density (N_t) by the

equation: $N_t = 2\varepsilon\varepsilon_0 V_{TFL}/eL^2$, where ε, ε_0, e and L represent dielectric constant, vacuum permittivity, element charge, and thickness of perovskite films, respectively. The control device delivered a V_{TFL} of 0.237 V and N_t of 5.73×10^{15} cm^{-3}, while the PSMA enabled devices to show a much smaller V_{TFL} of 0.121 V and N_t of 2.93×10^{15} cm^{-3} (**Figure S7**).[33] Lower trap density can reduce the nonradiative recombination of charge carriers. These results further verify the effectiveness of our passivation strategy.

The ideality factor (n) is usually used to describe the recombination loss in the perovskite. Typically, n = 1 denotes that radiative recombination completely dominates the recombination dynamics, and n = 2 represents nonradiative recombination through imperfections and traps dominates.[34] As shown in **Figure S8**, the light intensity-dependent V_{oc} variation was investigated. The PSMA-treated device showed an n of 1.29, which was quite smaller than that of the control device (1.50), indicating that the trap/defect-induced recombination was effectively suppressed.[35] Besides, electrochemical impedance spectroscopy (EIS) was measured, and the Nyquist plots were displayed in **Figure S9**. Specifically, the semicircles contain the information on the series resistance (R_s) and the recombination resistance (R_{rec}) for devices that are empirically associated with charge transfer and recombination, respectively.[36] Obviously, the PSMA-treated device showed smaller R_s and larger R_{rec}, implying that the nonradiative recombination was significantly inhibited.

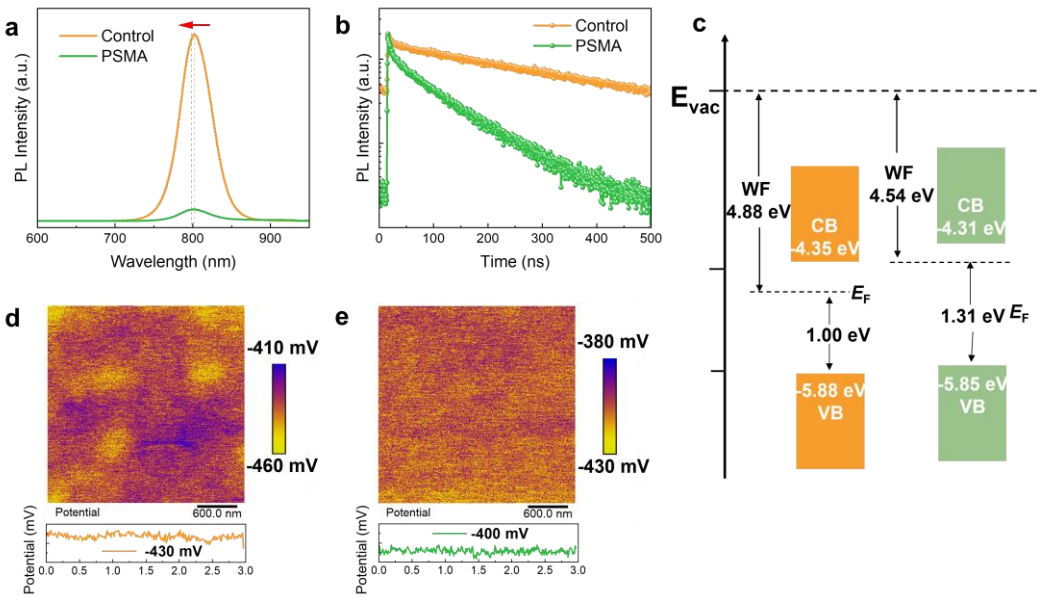

Figure 3. (a) PL, (b) TRPL spectra, and (c) energy level of control and PSMA perovskite films. KPFM images of (d) control and (e) PSMA perovskite films. The bottom curves represent the surface potentials.

2.3 Working mechanism of PSMA IPSCs

According to the above results, PSMA is mainly distributed on the perovskite surface and is supposed to penetrate the perovskite grain boundary near the top surface with a graded distribution. A reasonable working mechanism for the PSMA-regulated IPSCs performance improvement could be proposed and illustrated in **Figure 4**. It mainly contains several aspects. First, the interactions between perovskite and PSMA (especially for the interaction between -C≡N and -C=O groups with PbI_2) are fully conducted across the surface and extended to the grain boundary near the top surface. The -C≡N and -C=O groups firmly bond with the undercoordinated Pb^{2+} of perovskite by Lewis base sites, resulting in reduced trap states and suppressed nonradiative recombination. In addition, the increased surface potential and up-shifted E_F with PSMA contribute to a more n-type perovskite surface, which is beneficial for fast electron transport. Moreover, the smooth perovskite surface with low surface potential variations by PY-IT significantly improved electron transfer with reduced recombination. Notably, ring fusion endowed strong planarity and polymer nature for PY-IT makes it capable of orderly self-arranging at the upper surface of perovskite; and its rotatable linker demonstrates the applicability of PSMA's inserting into grain boundaries as shown in **Figure 4**. Therefore, it is anticipated that electron can transport along the highway of PSMA among the boundaries and electron transport can be enhanced between PSMA and PCBM due to their strong π-π interaction. Furthermore, the reduced δ-$FAPbI_3$ by PSMA is suggested to increase the inherent phase stability of perovskite structure. As a result, this strategy helps to minimize the energy loss at the interface between perovskite and ETL, thus improving the performance of IPSCs.

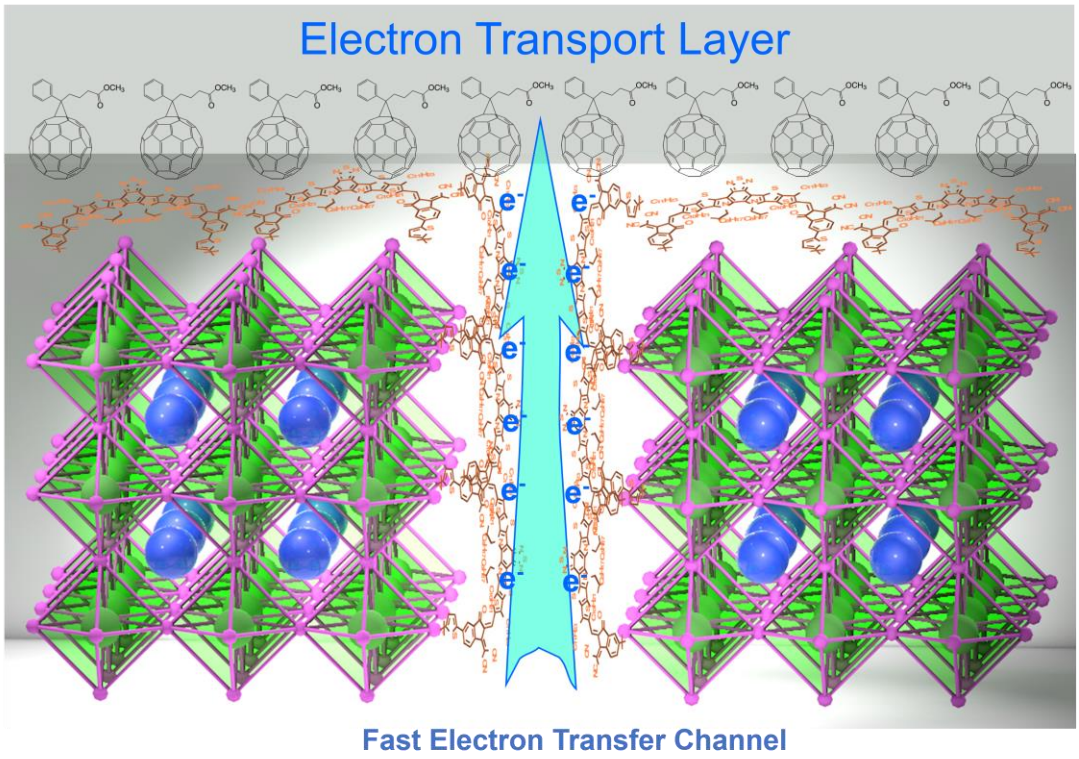

Figure 4. Mechanism of the defect passivation and improved electron transport properties with PSMA.

2.4 Device performances of PSMA IPSCs

To investigate the effect of defect passivation and regulated electron transport on device performance, IPSCs with the structure of ITO/2PACz/$Cs_{0.05}(FA_{0.98}MA_{0.02})_{0.95}Pb(I_{0.98}Br_{0.02})_3$/PCBM/BCP/Ag were fabricated, where PSMA was coated onto the perovskite surface as an interlayer (**Figure 5a**). As the typical *J-V* curves of the devices shown in **Figure 5b**. The control device delivered a PCE of 21.98% with V_{oc} of 1.12 V, J_{sc} of 24.14 mA/cm^2 and FF of 81%, whereas the champion PSMA-based PSC achieved a high PCE of 23.57% with V_{oc} of 1.15 V, J_{sc} of 24.37 mA/cm^2 and FF of 84%. The concentration of PSMA was optimized as 1 mg/ml in chlorobenzene (**Figure S10**). In a lower concentration, the introduction of PSMA can contribute to effective passivation and interfacial charge transfer, which increased the V_{oc} and FF. And the concentration is optimized at 1 mg/ml for a high efficiency of 23.57%. However, when the concentration is going higher, the lower electron mobility of PY-IT (compared with PCBM) may cause undesirable energy loss which causes the drop of FF and J_{sc}.[37] To our best knowledge, the PCE of this PSMA-based IPSCs is competed with the highest PCEs of other non-fullerene acceptors (small molecule counterparts) incorporated IPSCs (**Figure S11**). A slight improvement in J_{sc} was observed, while V_{oc} and FF were significantly enhanced with PSMA, which could be ascribed to the reduced traps and facilitated electron transport. The external quantum efficiency (EQE) was conducted to evaluate the accuracy of J_{sc}, as shown in **Figure 5c**, the control IPSC exhibited an integrated J_{sc} of 23.50 mA/cm^2, whereas the PSMA-based IPSCs delivered a slightly higher integrated J_{sc} up to 23.72 mA/cm^2, in accordance with the results from *J-V* curves. Additionally, devices incorporating PSMA exhibited negligible hysteresis (**Figure S12**). Under the bias voltage of 1.00 V, the stabilized output efficiency of PSMA-based device was 22.86%, which was higher than that of the control device (20.52% under a bias voltage of 0.98 V)(**Figure 4d**). **Figure S10** displayed the histogram of PCE distribution, suggesting excellent reproducibility of PSMA-based IPSCs.

To further prove the applicability of this strategy, narrow-bandgap ($Cs_{0.1}FA_{0.6}MA_{0.3}Pb_{0.5}Sn_{0.5}I_3$, 1.25 eV) IPSCs were fabricated.[38] As shown in **Figure S13**, the champion efficiency of Pb-Sn-based IPSC with PSMA was close to 20%, while that of the control device was 17.38%. The improved efficiency is ascribed to the enhanced V_{oc}, J_{sc}, and FF, indicating that trap states in the device are reduced, which further confirms the effective passivation by PSMA. Moreover, it is quite interesting that the PY-IT itself can work effectively as ETL for IPSCs. As shown in **Figure S14**, the PY-IT (ETL) shows an efficiency of 14.56% with a V_{oc} of 0.88 V, a J_{sc}, of 23.94 mA/cm^2 and FF of 0.69.

In addition to the improved efficiency, the stability of devices was also assessed. Upon storage in N_2, the device is storage with light illumination and open circuit. The PSMA-based device can retain 86% of its initial efficiency without encapsulation after 1000 h, while the control device dropped to 78% after only 400 h (**Figure 4e**). Furthermore, the operational stability was measured under continuous 1 sun illumination (white LED lamp) under maximum power point (MPP) tracking. In this situation, the ion migration in the device is accelerated by both light and applied bias.[39] The encapsulated PSMA-based device retained 80% of its initial efficiency for 1000 h under MPP tracking in the ambient atmosphere (25□ and 65% RH). In contrast, the control device showed noticeable degradation and retained 50% of its initial value after MPP tracking for 750 h (**Figure 4f**). Accordingly, the surface reconstruction of perovskite film by PSMA successfully achieves enhanced device stability.[40]

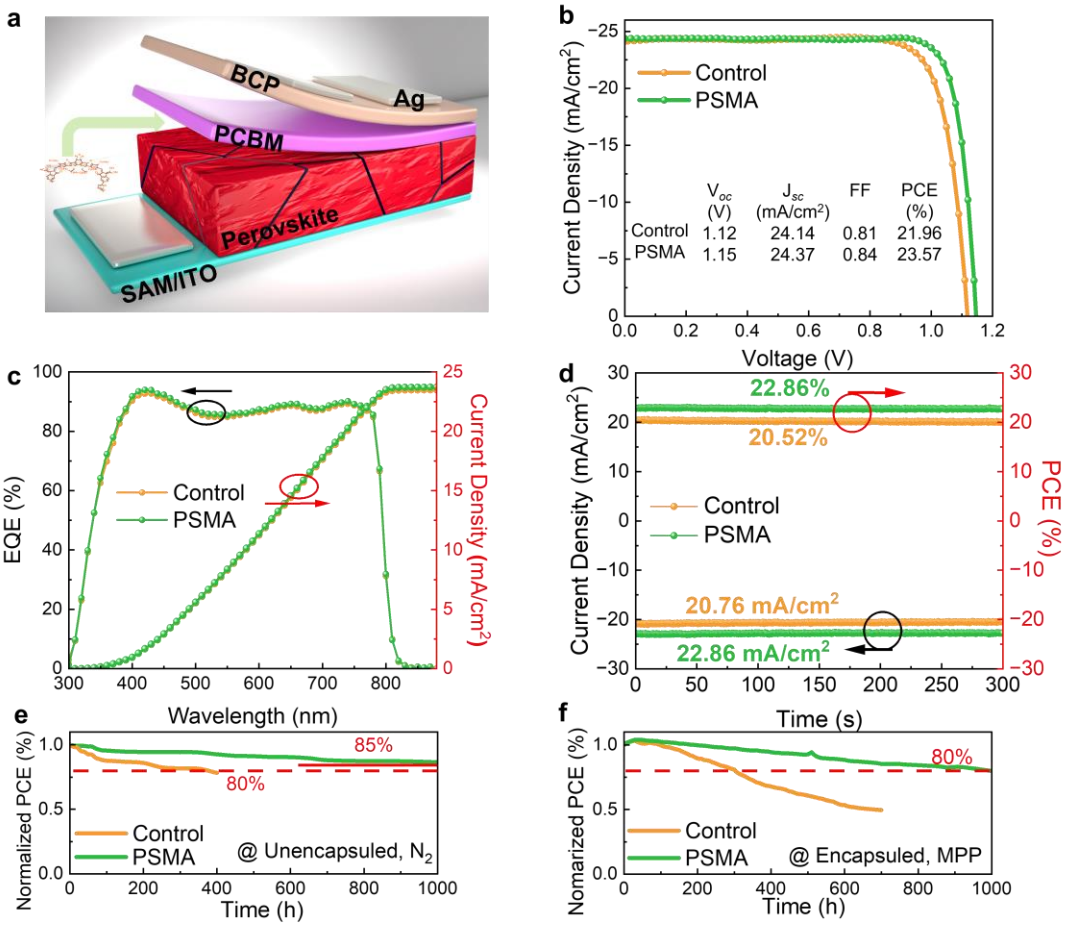

Figure 5. (a) Device structure of the IPSCs (b) *J-V* curves, (c) EQE curves, (d) stabilized output curves, (e) long-term storage stability in N_2 atmosphere, and (f) operational stability under MPP tracking of control and PSMA perovskite devices.

3. Conclusion

In conclusion, to avoid the potential disadvantages of small molecules, a PSMA named PY-IT was incorporated into the perovskite/ETL interface as the modulator. Detailed characterizations revealed that PSMAs were located on the perovskite top surface and grain boundaries, thus reducing trap states while constructing n-type surface and charge-transport-friendly perovskite orientation. Due to the effective interfacial modulation of PSMA, the champion devices delivered PCEs of 23.57% and 19.62% for 1.53 eV and 1.25 eV bandgap IPSCs, respectively. Moreover, the incorporation of PSMA enhanced the storage and operational stability of IPSCs, which retained 86% and 80% of their initial PCEs. Taken together, our work provides a novel pathway to optimize the top surface of perovskites with high efficiency and operational reliability.

Acknowledgements

G. Li acknowledges the support from Research Grants Council of Hong Kong (Project Nos 15320216, 15221320, C5037-18G), RGC Senior Research Fellowship Scheme (SRFS2122-5S04), National Natural Science Foundation of China (51961165102), Shenzhen Science and Technology Innovation Commission (JCYJ20200109105003940, SGDX2019081623220944), the Hong Kong Polytechnic University Internal Research Funds: Sir Sze-yuen Chung Endowed Professorship Fund (8-8480), RISE (1-CDA5), 1-W15V, and Guangdong-Hong Kong-Macao Joint Laboratory for Photonic-Thermal-Electrical Energy Materials and Devices (GDSTC No. 2019B121205001). C. C. thanks the National Natural Science Foundation of China (Grant No. 91963129), the Guangdong Provincial Key Laboratory of Energy Materials for Electric Power (Grant No. 2018B030322001), the Student Innovation Training Program (Grant Nos. 2021S07) from Southern University of Science and Technology (SUSTech), and the Special Funds for the Cultivation of Guangdong College Students' Scientific and Technological Innovation (pdjh2022c0003& pdjh2022c0005).

Author Contribution

D. Li and Y. Huang contributed equal to this work.

D. Li: Conceptualization, Investigation, Formal Analysis, Writing the Original Draft.

Y. Huang: Investigation, Formal Analysis and Writing the Original Draft.

R. Ma: Conceptualization, Investigation, Writing- Reviewing and Editing

H. Liu: Investigation

Q. Liang: Visualization, Investigation

Y. Han: Investigation

Z. Ren.: Data Curation

K. Liu: Investigation

P. Fong: Investigation

Z. Zhang: Investigation

Q. Lian: Investigation

X. Lu: Resources

C. Cheng: Funding Acquisition Supervision and Writing- Reviewing and Editing

G. Li: Funding Acquisition, Conceptualization, Supervision and Writing- Reviewing and Editing, Project Administration.

All authors revised the manuscript.

Conflict of interest

Authors declare no conflict of interests.

Reference:

[1] a) Y. Zhao, F. Ma, Z. Qu, S. Yu, T. Shen, H. X. Deng, X. Chu, X. Peng, Y. Yuan, X. Zhang, J. You, *Science* **2022**, 377, 531; b) J. Jeong, M. Kim, J. Seo, H. Lu, P. Ahlawat, A. Mishra, Y. Yang, M. A. Hope, F. T. Eickemeyer, M. Kim, Y. J. Yoon, I. W. Choi, B. P. Darwich, S. J. Choi, Y. Jo, J. H. Lee, B. Walker, S. M. Zakeeruddin, L. Emsley, U. Rothlisberger, A. Hagfeldt, D. S. Kim, M. Gratzel, J. Y. Kim, *Nature* **2021**, 592, 381; c) M. Kim, J. Jeong, H. Lu, T. K. Lee, F. T. Eickemeyer, Y. Liu, I. W. Choi, S. J. Choi, Y. Jo, H. B. Kim, S. I. Mo, Y. K. Kim, H. Lee, N. G. An, S. Cho, W. R. Tress, S. M. Zakeeruddin, A. Hagfeldt, J. Y. Kim, M. Gratzel, D. S. Kim, *Science* **2022**, 375, 302; d) Y. Rong, Y. Hu, A. Mei, H. Tan, M. I. Saidaminov, S. I. Seok, M. D. McGehee, E. H. Sargent, H. Han, *Science* **2018**, 361, 1214.

[2] a) T. Liu, K. Chen, Q. Hu, R. Zhu, Q. Gong, *Adv. Energy Mater.* **2016**, 6, 1600457; b) X. Lin, D. Cui, X. Luo, C. Zhang, Q. Han, Y. Wang, L. Han, *Energy Environ. Sci.* **2020**, 13, 3823.

[3] a) X. Li, W. Zhang, X. Guo, C. Lu, J. Wei, J. Fang, *Science* **2022**, 375, 434; b) F. Li, X. Deng, F. Qi, Z. Li, D. Liu, D. Shen, M. Qin, S. Wu, F. Lin, S. H. Jang, J. Zhang, X. Lu, D. Lei, C. S. Lee, Z. Zhu, A. K. Jen, *J. Am. Chem. Soc.* **2020**, 142, 20134; c) R. Azmi, E. Ugur, A. Seitkhan, F. Aljamaan, A. S. Subbiah, J. Liu, G. T. Harrison, M. I. Nugraha, M. K. Eswaran, M. Babics, Y. Chen, F. Xu, T. G. Allen, A. U. Rehman, C. L. Wang, T. D. Anthopoulos, U. Schwingenschlogl, M. De Bastiani, E. Aydin, S. De Wolf, *Science* **2022**, 376, 73; d) Z. Li, B. Li, X. Wu, S. A. Sheppard, S. Zhang, D. Gao, N. J. Long, Z. Zhu, *Science* **2022**, 376, 416; e) A. Mei, Y. Sheng, Y. Ming, Y. Hu, Y. Rong, W. Zhang, S. Luo, G. Na, C. Tian, X. Hou, Y. Xiong, Z. Zhang, S. Liu, S. Uchida, T.-W. Kim, Y. Yuan, L. Zhang, Y. Zhou, H. Han, *Joule* **2020**, 4, 2646.

[4] a) B. Chen, P. N. Rudd, S. Yang, Y. Yuan, J. Huang, *Chem. Soc. Rev.* **2019**, 48, 3842; b) D. Li, W. Kong, H. Zhang, D. Wang, W. Li, C. Liu, H. Chen, W. Song, F. Gao, A. Amini, B. Xu, S. Li, C. Cheng, *ACS Appl. Mater. Interfaces* **2020**, 12, 20103; c) A. Fakharuddin, L. Schmidt-Mende, G. Garcia-Belmonte, R. Jose, I. Mora-Sero, *Adv. Energy Mater.* **2017**, 7, 1700623; d) X. Zheng, J. Troughton, N. Gasparini, Y. Lin, M. Wei, Y. Hou, J. Liu, K. Song, Z. Chen, C. Yang, B. Turedi, A. Y. Alsalloum, J. Pan, J. Chen, A. A. Zhumekenov, T. D. Anthopoulos, Y. Han, D. Baran, O. F. Mohammed, E. H. Sargent, O. M. Bakr, *Joule* **2019**, 3, 1963; e) M. Zhang, Q. Chen, R. Xue, Y. Zhan, C. Wang, J. Lai, J. Yang, H. Lin, J. Yao, Y. Li, L. Chen, Y. Li, *Nat. Commun.* **2019**, 10, 4593; f) S. Wang, H. Chen, J. Zhang, G. Xu, W. Chen, R. Xue, M. Zhang, Y. Li, Y. Li, *Adv. Mater.* **2019**, 31, e1903691; g) M. Zhang, Q. Chen, R. Xue, Y. Zhan, C. Wang, J. Lai, J. Yang, H. Lin, J. Yao, Y. Li, L. Chen, Y. Li, *Nat Commun* **2019**, 10, 4593.

[5] a) Y. Yao, C. Cheng, C. Zhang, H. Hu, K. Wang, S. De Wolf, *Adv. Mater.* **2022**, 34, e2203794; b) T. H. Han, S. Tan, J. Xue, L. Meng, J. W. Lee, Y. Yang, *Adv. Mater.* **2019**, 31, e1803515.

[6] a) L. Fu, H. Li, L. Wang, R. Yin, B. Li, L. Yin, *Energy Environ. Sci.* **2020**, 13, 4017; b) F. Gao, Y. Zhao, X. Zhang, J. You, *Adv. Energy Mater.* **2019**, 10, 1902650; c) S. Cacovich, G. Vidon, M. Degani, M. Legrand, L. Gouda, J. B. Puel, Y. Vaynzof, J. F. Guillemoles, D. Ory, G. Grancini, *Nat. Commun.* **2022**, 13, 2868; d) W. Chen, S. Liu, Q. Li, Q. Cheng, B. He, Z. Hu, Y. Shen, H. Chen, G. Xu, X. Ou, H. Yang, J. Xi, Y. Li, Y. Li, *Adv. Mater.* **2022**, 34, e2110482.

[7] a) X. Luo, Z. Shen, Y. Shen, Z. Su, X. Gao, Y. Wang, Q. Han, L. Han, *Adv. Mater.* **2022**, 34, e2202100; b) M. Qin, J. Cao, T. Zhang, J. Mai, T.-K. Lau, S. Zhou, Y. Zhou, J. Wang, Y.-J. Hsu, N. Zhao, J. Xu, X. Zhan, X. Lu, *Adv. Energy Mater.* **2018**, 8, 1703399; c) Q. Yang, X. Liu, S. Yu, Z. Feng, L. Liang, W. Qin, Y. Wang, X. Hu, S. Chen, Z. Feng, G. Hou, K. Wu, X. Guo, C. Li, *Energy Environ. Sci.* **2021**, 14, 6536; d) Q. Hu, W. Chen, W. Yang, Y. Li, Y. Zhou, B. W. Larson, J. C. Johnson, Y.-H. Lu, W. Zhong, J. Xu, L. Klivansky, C. Wang, M. Salmeron, A. B. Djurišić, F. Liu, Z. He, R. Zhu, T. P. Russell, *Joule* **2020**, 4, 1575; e) X. Liu, X. Li, Y. Zou, H. Liu, L. Wang, J. Fang, C. Yang, *J. Mater. Chem. A* **2019**, 7, 3336; f) G. Yang, P. Qin, G. Fang, G. Li, *Solar RRL* **2018**, 2, 1800055; g) J. Zhang, J. Guan, Y. Zhang, S. Qin, Q. Zhu, X. Kong,

Q. Ma, X. Li, L. Meng, Y. Yi, J. Zheng, Y. Li, *J. Phys. Chem. Lett.* **2022**, 13, 8816; h) G. Han, Y. Yi, *Acc. Chem. Res.* **2022**, 55, 869.
[8] W. Li, D. Liu, T. Wang, *Adv. Funct. Mater.* **2021**, 31, 2104552.
[9] a) Z. G. Zhang, Y. Li, *Angew. Chem. Int. Ed.* **2021**, 60, 4422; b) Z. G. Zhang, Y. Yang, J. Yao, L. Xue, S. Chen, X. Li, W. Morrison, C. Yang, Y. Li, *Angew. Chem. Int. Ed.* **2017**, 56, 13503.
[10] a) P. L. Qin, G. Yang, Z. W. Ren, S. H. Cheung, S. K. So, L. Chen, J. Hao, J. Hou, G. Li, *Adv. Mater.* **2018**, 30, e1706126; b) Q. Cheng, H. Chen, F. Yang, Z. Chen, W. Chen, H. Yang, Y. Shen, X. M. Ou, Y. Wu, Y. Li, Y. Li, *Angew. Chem. Int. Ed.* **2022**, 61, e202210613.
[11] a) C. Cui, Y. Li, Y. Li, *Adv. Energy Mater.* **2017**, 7, 1601251; b) T. Wu, Y. Wang, X. Li, Y. Wu, X. Meng, D. Cui, X. Yang, L. Han, *Adv. Energy Mater.* **2019**, 9, 1803766.
[12] a) Z. Luo, T. Liu, R. Ma, Y. Xiao, L. Zhan, G. Zhang, H. Sun, F. Ni, G. Chai, J. Wang, C. Zhong, Y. Zou, X. Guo, X. Lu, H. Chen, H. Yan, C. Yang, *Adv. Mater.* **2020**, 32, e2005942; b) J. Wang, Y. Cui, Y. Xu, K. Xian, P. Bi, Z. Chen, K. Zhou, L. Ma, T. Zhang, Y. Yang, Y. Zu, H. Yao, X. Hao, L. Ye, J. Hou, *Adv. Mater.* **2022**, 34, e2205009; c) R. Ma, K. Zhou, Y. Sun, T. Liu, Y. Kan, Y. Xiao, T. A. Dela Peña, Y. Li, X. Zou, Z. Xing, Z. Luo, K. S. Wong, X. Lu, L. Ye, H. Yan, K. Gao, *Matter* **2022**, 5, 725; d) K. Hu, C. Zhu, S. Qin, W. Lai, J. Du, L. Meng, Z. Zhang, Y. Li, *Sci. Bull.* **2022**, 67, 2096.
[13] a) E. Aydin, M. De Bastiani, S. De Wolf, *Adv. Mater.* **2019**, 31, e1900428; b) Y. Huang, T. Liu, B. Wang, J. Li, D. Li, G. Wang, Q. Lian, A. Amini, S. Chen, C. Cheng, G. Xing, *Adv. Mater.* **2021**, 33, e2102816.
[14] a) D. Li, Y. Huang, G. Wang, Q. Lian, R. Shi, L. Zhang, X. Wang, F. Gao, W. Kong, B. Xu, C. Cheng, S. Li, *J. Mater. Chem. A* **2021**, 9, 12746; b) X. Zheng, Y. Hou, C. Bao, J. Yin, F. Yuan, Z. Huang, K. Song, J. Liu, J. Troughton, N. Gasparini, C. Zhou, Y. Lin, D.-J. Xue, B. Chen, A. K. Johnston, N. Wei, M. N. Hedhili, M. Wei, A. Y. Alsalloum, P. Maity, B. Turedi, C. Yang, D. Baran, T. D. Anthopoulos, Y. Han, Z.-H. Lu, O. F. Mohammed, F. Gao, E. H. Sargent, O. M. Bakr, *Nat. Energy* **2020**, 5, 131.
[15] Z. Xiong, X. Chen, B. Zhang, G. O. Odunmbaku, Z. Ou, B. Guo, K. Yang, Z. Kan, S. Lu, S. Chen, N. A. N. Ouedraogo, Y. Cho, C. Yang, J. Chen, K. Sun, *Adv. Mater.* **2022**, 34, e2106118.
[16] a) Y. Wang, T. Wu, J. Barbaud, W. Kong, D. Cui, H. Chen, X. Yang, L. Han, *Science* **2019**, 365, 687; b) S. H. Cho, J. Byeon, K. Jeong, J. Hwang, H. Lee, J. Jang, J. Lee, T. Kim, K. Kim, M. Choi, Y. S. Lee, *Adv. Energy Mater.* **2021**, 11, 2100555; c) H. Wang, F. Ye, J. Liang, Y. Liu, X. Hu, S. Zhou, C. Chen, W. Ke, C. Tao, G. Fang, *Joule* **2022**, DOI: 10.1016/j.joule.2022.10.001.
[17] a) K. Huang, Y. Peng, Y. Gao, J. Shi, H. Li, X. Mo, H. Huang, Y. Gao, L. Ding, J. Yang, *Adv. Energy Mater.* **2019**, 9, 1901419; b) W. Chen, H. Chen, G. Xu, R. Xue, S. Wang, Y. Li, Y. Li, *Joule* **2019**, 3, 191.
[18] H. Choi, X. Liu, H. I. Kim, D. Kim, T. Park, S. Song, *Adv. Energy Mater.* **2021**, 11, 2003829.
[19] J. Zhang, H. Yu, *J. Mater. Chem. A* **2021**, 9, 4138.
[20] a) X. Zhou, L. Zhang, J. Yu, D. Wang, C. Liu, S. Chen, Y. Li, Y. Li, M. Zhang, Y. Peng, Y. Tian, J. Huang, X. Wang, X. Guo, B. Xu, *Adv. Mater.* **2022**, 34, e2205809; b) L. Wang, L. Fu, B. Li, H. Li, L. Pan, B. Chang, L. Yin, *Solar RRL* **2021**, 5, 2000720; c) T. H. Han, J. W. Lee, C. Choi, S. Tan, C. Lee, Y. Zhao, Z. Dai, N. De Marco, S. J. Lee, S. H. Bae, Y. Yuan, H. M. Lee, Y. Huang, Y. Yang, *Nat. Commun.* **2019**, 10, 520; d) J. Jiang, Q. Wang, Z. Jin, X. Zhang, J. Lei, H. Bin, Z.-G. Zhang, Y. Li, S. F. Liu, *Adv. Energy Mater.* **2018**, 8, 1701757.
[21] a) X. Deng, F. Li, Q. Wang, D. Liu, F. Lin, D. Shen, D. Lei, Y.-K. Peng, Z. Zhu, A. K. Y. Jen, *Matter* **2021**, 4, 3301; b) S. Bai, P. Da, C. Li, Z. Wang, Z. Yuan, F. Fu, M. Kawecki, X. Liu, N. Sakai, J. T. Wang, S. Huettner, S. Buecheler, M. Fahlman, F. Gao, H. J. Snaith, *Nature* **2019**, 571, 245.

[22] a) Y. Liu, S. Akin, A. Hinderhofer, F. T. Eickemeyer, H. Zhu, J. Y. Seo, J. Zhang, F. Schreiber, H. Zhang, S. M. Zakeeruddin, A. Hagfeldt, M. I. Dar, M. Gratzel, *Angew. Chem. Int. Ed.* **2020**, 59, 15688; b) J. Zhang, X. Jiang, X. Liu, X. Guo, C. Li, *Adv. Funct. Mater.* **2022**, 32, 2204642; c) T. Du, T. J. Macdonald, R. X. Yang, M. Li, Z. Jiang, L. Mohan, W. Xu, Z. Su, X. Gao, R. Whiteley, C. T. Lin, G. Min, S. A. Haque, J. R. Durrant, K. A. Persson, M. A. McLachlan, J. Briscoe, *Adv. Mater.* **2022**, 34, e2107850.
[23] T. Liu, T. Yang, R. Ma, L. Zhan, Z. Luo, G. Zhang, Y. Li, K. Gao, Y. Xiao, J. Yu, X. Zou, H. Sun, M. Zhang, T. A. Dela Peña, Z. Xing, H. Liu, X. Li, G. Li, J. Huang, C. Duan, K. S. Wong, X. Lu, X. Guo, F. Gao, H. Chen, F. Huang, Y. Li, Y. Li, Y. Cao, B. Tang, H. Yan, *Joule* **2021**, 5, 914.
[24] a) S. R. Pering, W. Deng, J. R. Troughton, P. S. Kubiak, D. Ghosh, R. G. Niemann, F. Brivio, F. E. Jeffrey, A. B. Walker, M. S. Islam, T. M. Watson, P. R. Raithby, A. L. Johnson, S. E. Lewis, P. J. Cameron, *J. Mater. Chem. A* **2017**, 5, 20658; b) A. Z. Chen, B. J. Foley, J. H. Ma, M. R. Alpert, J. S. Niezgoda, J. J. Choi, *J. Mater. Chem. A* **2017**, 5, 7796.
[25] M. Qin, P. F. Chan, X. Lu, *Adv. Mater.* **2021**, 33, e2105290.
[26] a) F. Zhang, W. Shi, J. Luo, N. Pellet, C. Yi, X. Li, X. Zhao, T. J. S. Dennis, X. Li, S. Wang, Y. Xiao, S. M. Zakeeruddin, D. Bi, M. Gratzel, *Adv. Mater.* **2017**, 29; b) Q. He, M. Worku, H. Liu, E. Lochner, A. J. Robb, S. Lteif, J. S. R. Vellore Winfred, K. Hanson, J. B. Schlenoff, B. J. Kim, B. Ma, *Angew. Chem. Int. Ed.* **2021**, 60, 2485.
[27] D. Yang, X. Zhang, K. Wang, C. Wu, R. Yang, Y. Hou, Y. Jiang, S. Liu, S. Priya, *Nano Lett.* **2019**, 19, 3313.
[28] a) Y. Zhan, F. Yang, W. Chen, H. Chen, Y. Shen, Y. Li, Y. Li, *Adv. Mater.* **2021**, 33, e2105170; b) G. Yang, Z. Ren, K. Liu, M. Qin, W. Deng, H. Zhang, H. Wang, J. Liang, F. Ye, Q. Liang, H. Yin, Y. Chen, Y. Zhuang, S. Li, B. Gao, J. Wang, T. Shi, X. Wang, X. Lu, H. Wu, J. Hou, D. Lei, S. K. So, Y. Yang, G. Fang, G. Li, *Nat. Photonics* **2021**, 15, 681; c) Q. Jiang, J. Tong, Y. Xian, R. A. Kerner, S. P. Dunfield, C. Xiao, R. A. Scheidt, D. Kuciauskas, X. Wang, M. P. Hautzinger, R. Tirawat, M. C. Beard, D. P. Fenning, J. J. Berry, B. W. Larson, Y. Yan, K. Zhu, *Nature* **2022**, 611, 278; d) C. Bi, Q. Wang, Y. Shao, Y. Yuan, Z. Xiao, J. Huang, *Nat. Commun.* **2015**, 6, 7747; e) Y. Shao, Z. Xiao, C. Bi, Y. Yuan, J. Huang, *Nat. Commun.* **2014**, 5, 5784.
[29] F. Wang, S. Bai, W. Tress, A. Hagfeldt, F. Gao, *npj Flexible Electronics* **2018**, 2, 22.
[30] W. Chen, Y. Shi, Y. Wang, X. Feng, A. B. Djurišić, H. Y. Woo, X. Guo, Z. He, *Nano Energy* **2020**, 68, 104363.
[31] S. Xiong, Z. Hou, S. Zou, X. Lu, J. Yang, T. Hao, Z. Zhou, J. Xu, Y. Zeng, W. Xiao, W. Dong, D. Li, X. Wang, Z. Hu, L. Sun, Y. Wu, X. Liu, L. Ding, Z. Sun, M. Fahlman, Q. Bao, *Joule* **2021**, 5, 467.
[32] a) Y. Sun, R. Ma, Y. Kan, T. Liu, K. Zhou, P. Liu, J. Fang, Y. Chen, L. Ye, C. Ma, H. Yan, K. Gao, *Macromol. Rapid Commun.* **2022**, 43, e2200139; b) M. Kataria, H. D. Chau, N. Y. Kwon, S. H. Park, M. J. Cho, D. H. Choi, *ACS Energy Lett.* **2022**, 7, 3835.
[33] Y. Han, T. Zuo, K. He, L. Yang, S. Zhan, Z. Liu, Z. Ma, J. Xu, Y. Che, W. Zhao, N. Yuan, J. Ding, J. Sun, X. He, S. Liu, *Materials Today* **2022**, 61, 54.
[34] D. Glowienka, Y. Galagan, *Adv. Mater.* **2021**, 34, 2105920.
[35] P. Caprioglio, C. M. Wolff, O. J. Sandberg, A. Armin, B. Rech, S. Albrecht, D. Neher, M. Stolterfoht, *Adv. Energy Mater.* **2020**, 10, 2000502.
[36] a) L. Xiong, M. Qin, C. Chen, J. Wen, G. Yang, Y. Guo, J. Ma, Q. Zhang, P. Qin, S. Li, G. Fang, *Adv. Funct. Mater.* **2018**, 28, 1706276; b) Y. Han, H. Zhao, C. Duan, S. Yang, Z. Yang, Z. Liu, S. Liu, *Adv. Funct. Mater.* **2020**, 30, 1909972.
[37] a) E. von Hauff, V. Dyakonov, J. Parisi, *Solar Energy Materials and Solar Cells* **2005**, 87, 149; b) Y. Sun, R. Ma, Y. Kan, T. Liu, K. Zhou, P. Liu, J. Fang, Y. Chen, L. Ye, C. Ma, H. Yan, K. Gao, *Macromol. Rapid. Commun.* **2022**, 43, e2200139.
[38] S. Hu, K. Otsuka, R. Murdey, T. Nakamura, M. A. Truong, T. Yamada, T. Handa, K.

Matsuda, K. Nakano, A. Sato, K. Marumoto, K. Tajima, Y. Kanemitsu, A. Wakamiya, *Energy Environ. Sci.* **2022**, 15, 2096.
[39] a) N. Li, X. Niu, Q. Chen, H. Zhou, *Chem. Soc. Rev.* **2020**, 49, 8235; b) K. Domanski, E. A. Alharbi, A. Hagfeldt, M. Grätzel, W. Tress, *Nature Energy* **2018**, 3, 61.
[40] a) Z. Zhu, Y. Bai, X. Liu, C. C. Chueh, S. Yang, A. K. Jen, *Adv. Mater.* **2016**, 28, 6478; b) J. Wang, J. Li, Y. Zhou, C. Yu, Y. Hua, Y. Yu, R. Li, X. Lin, R. Chen, H. Wu, H. Xia, H. L. Wang, *J. Am. Chem. Soc.* **2021**, 143, 7759; c) G. Wang, R. Xu, H. Zhu, Y. Li, T. Liu, Z. Lin, M. Hu, Z. Xing, J. Gao, S. Yang, *Solar RRL* **2022**, 6, 2200559.

TOC

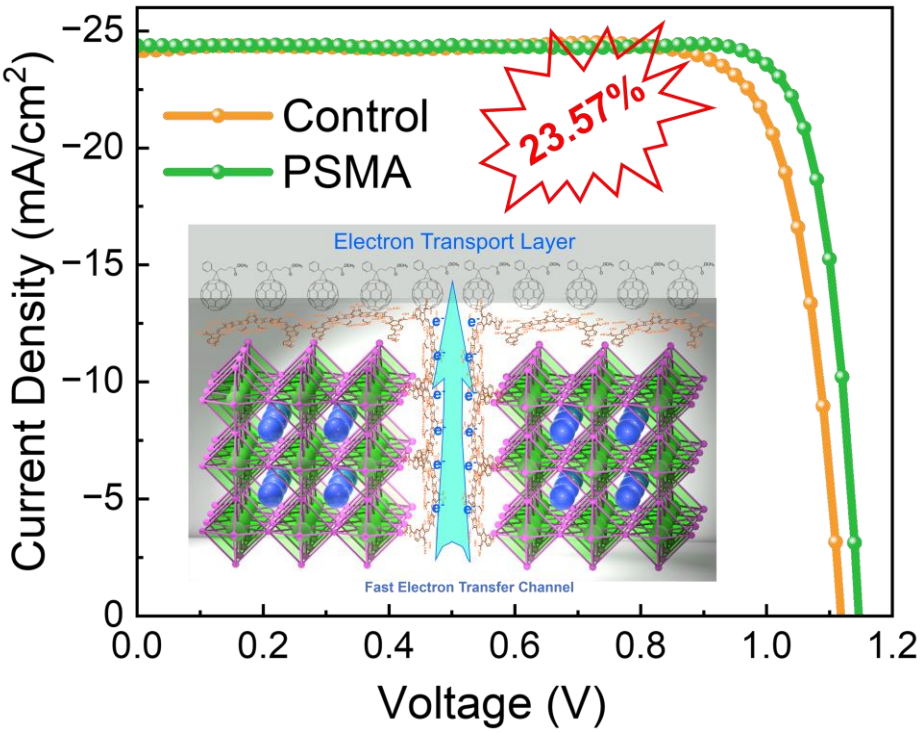

In this work, a novel strategy of applying polymerized small molecular acceptor to high-efficiency inverted perovskite solar cell is proposed and proven effective by the celebrity material PY-IT. Via the bi-passivation effect and additional electron transport channels, 23.57% PCE is obtained, as well as a decent operational stability.